Quaternary Science Reviews 266 (2021) 107074

Contents lists available at ScienceDirect

Quaternary Science Reviews

journal homepage: www.elsevier.com/locate/quascirev

Distal ash fall from the mid-Holocene eruption of Mount Hudson (H2) discovered in the Falkland Islands: New possibilities for Southern Hemisphere archive synchronisation

Panayiotis Panaretos [a, b, *], Paul G. Albert [c], Zoë A. Thomas [a, b, *], Chris S.M. Turney [a, b], Charles R. Stern [d], G. Jones [c], Alan N. Williams [e, f], Victoria C. Smith [g], Alan G. Hogg [h], Christina J. Manning [i]

[a] Chronos [14] Carbon-Cycle Facility, Mark Wainwright Analytical Centre, University of New South Wales, Sydney, NSW, 2052, Australia
[b] Earth and Sustainability Science Research Centre (ESSRC), School of Biological, Earth and Environmental Sciences, University of New South Wales, Sydney, NSW, 2052, Australia
[c] Department of Geography, Faculty of Science and Engineering, Swansea University, Swansea, SA2 8PP, UK
[d] Department of Geological Sciences, University of Colorado, Boulder, CO 80309-0399, USA
[e] EMM Consulting Pty Ltd, 20 Chandos Street, St Leonards, NSW, 2065, Australia
[f] ARC Centre of Excellence for Australian Biodiversity and Heritage, School of Biological, Earth and Environmental Sciences, University of New South Wales, NSW, 2052, Australia
[g] Research Laboratory for Archaeology and History of Art (RLAHA), University of Oxford, Oxford, OX1 3TG, UK
[h] Carbon Dating Laboratory, School of Science, University of Waikato, Hamilton, New Zealand
[i] Department of Earth Sciences, Royal Holloway University of London, Egham, Surrey, TW20 0EX, UK

ARTICLE INFO

Article history:
Received 22 April 2021
Received in revised form
27 June 2021
Accepted 29 June 2021
Available online xxx

Handling Editor: Giovanni Zanchetta

Keywords:
South America
Cryptotephra
Tephrochronology
Patagonia
Southern volcanic zone
Hudson
South Atlantic
Southern Ocean
Antarctic

ABSTRACT

Cryptotephra deposits (microscopic volcanic ash) are important geochronological tools that can be used to synchronize records of past environmental change. Here we report a distal cryptotephra from a Holocene peat sequence (Canopus Hill) in the Falkland Islands, in the South Atlantic. Using geochemical analysis (major- and trace-element) of individual volcanic glass shards, we provide a robust correlation between this cryptotephra and the large mid-Holocene explosive eruption of Mt. Hudson in Patagonia, Chile (H2; ~3.9 ka cal BP). The occurrence of H2 as a cryptotephra in the Falkland Islands significantly increases the known distribution of this marker horizon to more than 1200 km from the volcano, a threefold increase of its previous known extent. A high-resolution radiocarbon chronology, based on terrestrial plant macrofossils, dates the H2 tephra to 4265 ± 65 cal yr BP, suggesting that the eruption may have occurred slightly earlier than previously reported. The refined age and new geochemical reference dataset will facilitate the identification of the H2 tephra in other distal locations. The high concentration of glass shards in our peat sequence indicates that the H2 tephra may extend well beyond the Falkland Islands and we recommend future studies search for its presence across the sub-Antarctic islands and Antarctic Peninsula as a potentially useful chronological marker.

1. Introduction

Volcanic ash (tephra) dispersed from explosive volcanic eruptions has become a principal geochronological tool for correlating environmental records (e.g., Alloway et al., 2013; Lane et al., 2017). The near instantaneous deposition of tephra over large distances and its often-unique chemical signature allows tephra layers to provide time-parallel marker horizons (isochrones) (Turney and Lowe, 2001). Tephra isochrones can be used to synchronize records of past environmental change between sites and represent one of the most robust and versatile dating methods (Lowe, 2011). The application of tephra isochrones has been extended to include microscopic ash deposits (cryptotephras) which have been found in

* Corresponding authors. Chronos [14]Carbon-Cycle Facility, Mark Wainwright Analytical Centre, University of New South Wales, Sydney, NSW, 2052, Australia.
E-mail addresses: pana.panaretos@gmail.com (P. Panaretos), z.thomas@unsw.edu.au (Z.A. Thomas).

https://doi.org/10.1016/j.quascirev.2021.107074
0277-3791/

distal areas thousands of kilometres from source volcanoes (e.g., Dugmore, 1989; Wastegård et al., 2000; Dunbar et al., 2017; Kearney et al., 2018; Smith et al., 2020).

Despite the value that tephrochronology offers as a powerful geochronological tool, the technique has been underutilized in many regions. One such area is the South Atlantic, a region that owing to the prevailing mid-latitude westerly airflow, is favourably positioned downwind from the major volcanic zones (AVZ and SVZ; Austral and Southern Volcanic Zones) of southern South America (Fig. 1). Explosive volcanism is known to have occurred frequently at numerous volcanoes along these zones throughout the Holocene, including Mts. Burney, Aguilera and Reclus within the AVZ and Mt. Hudson in the SVZ (Fig. 1a; Stern, 2008; Fontijn et al., 2014). Tephras from these volcanic centres have previously been identified in lakes and peat bogs throughout southern Patagonia (Killian et al., 2003; Weller et al., 2015; Fontijn et al., 2016; Del Carlo et al., 2018; Smith et al., 2019). Only a limited number of cryptotephra deposits originating from Patagonian explosive volcanism have previously been reported in peat bogs across the Southern Atlantic, including the Falkland Islands and South Georgia (Hall et al., 2001; Oppedal et al., 2018), with the most recently identified linked to eruptions at Mt. Burney (MB_1; 8.85–9.95 ka cal BP) and the Reclus Volcano (R_1; 14.76 ± 0.18 ka cal BP (Monteath et al., 2019; Stern et al., 2011).

Tephrochronology studies in this region offer potential for the alignment of proxy reconstructions investigating climate and environmental change, including Southern Hemisphere westerly wind flow (Kilian and Lamy, 2012; Moreno et al., 2014; Lamy et al., 2010). Unfortunately, few distal tephras (>100 km) have been described in this region and the precise ages and distribution of key marker horizons remain uncertain. Here we present the results of new tephrostratigraphic investigations of the Canopus Hill peat sequence in the Falkland Islands (Fig. 1b), with a focus on the provenance and significance of a mid-Holocene cryptotephra identified in the succession.

2. Study area and methods

2.1. The Falkland Islands and the Canopus Hill sequence

The Falkland Islands are situated in the South Atlantic, 540 km east of the South American coast. The islands lie in the central latitudinal belt of the southern westerly winds (SWW) and have high monthly and annual windspeeds (6–9 ms^{-1}) (Upton and Shaw, 2002; Clark and Wilson, 1992). Peat bogs cover more than ~85% of the Falkland Islands and are ideal archives to trap and preserve volcanic ash (Otley et al., 2008). The combination of the prevailing airflow and abundance of peat makes the Falkland Islands ideally positioned to receive and preserve tephras from the major volcanic zones in South America (Fig. 1). Observations of modern volcanic eruptions suggest Patagonian ash fall has been deposited over the Falkland Islands, including ash from the 1991 Hudson eruption plume (Scasso et al., 1994; Kratzman et al., 2010).

To investigate the presence of distal cryptotephra, a 1.6 m peat sequence was extracted with a D-section corer from an exposed Ericaceous–grass peatland on Canopus Hill (51.691° S, 57.785° W) outside Port Stanley. Previous research at this site recognised the input of exotic pollen and charcoal derived from South America (Turney et al., 2016), as well as a multi-proxy reconstruction of atmospheric circulation changes (Thomas et al., 2018).

2.2. Tephrostratigraphy

The Canopus Hill peat sequence contained no visible tephra layers. The sequence was sampled contiguously every 4 cm. Samples were oven-dried (60 °C), weighed into ceramic crucibles (0.2 g dry wt.) and then ashed at 550 °C to concentrate any present cryptotephra (Dugmore, 1989; Pilcher and Hall, 1992). The mineral

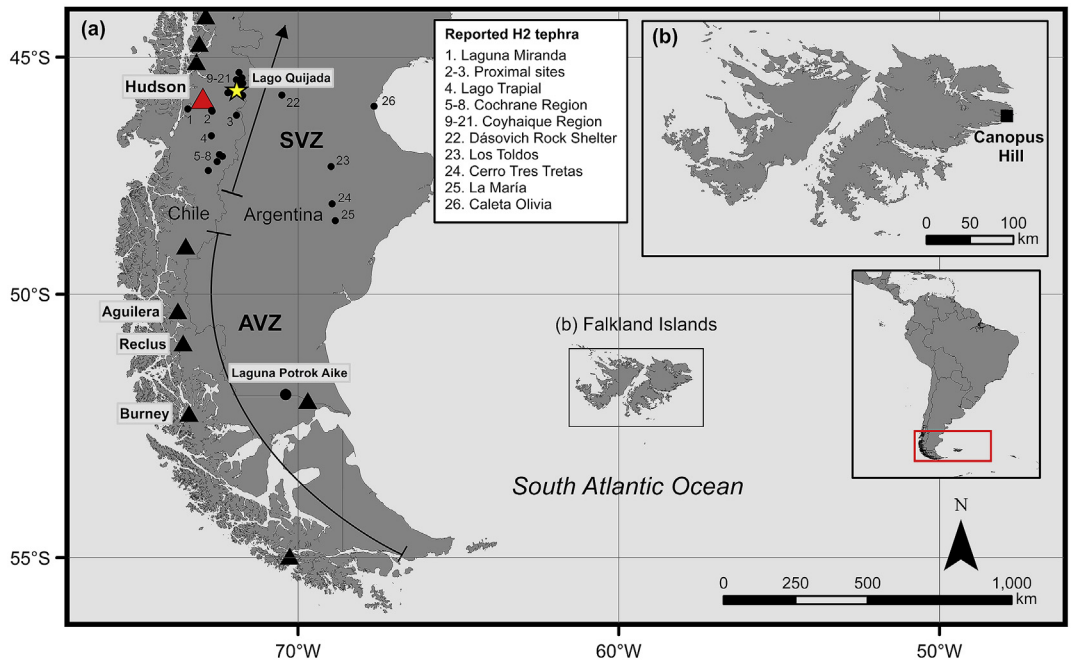

Fig. 1. Patagonia in southern South America depicting (a) the volcanoes (triangles) known to have erupted during the Holocene (Global Volcanism Program, 2020) from the Austral and Southern Volcanic Zones as defined by Stern (2004). (b) Location of the Falkland Islands and study site at Canopus Hill. Black dots represent locations where H2 tephra has been reported (Table S1). (1) Haberle and Lumley (1998); (2–3) Naranjo and Stern (1998); (4) Fagel et al. (2017); (5–8) Stern et al. (2016); Fagel et al. (2017); (9–21) Weller et al. (2015); Markgraf et al. (2007); Weller et al. (2018); Elbert et al. (2013); Weller and Stern (2018); (22) Stern et al. (2019); (23) Cardich (1985); Stern (1991); Naranjo and Stern (1998) (24) Paunero (1994); (25) Paunero (2000); (26) Zanchetta et al. (2021).

component was sieved (90–25 μm), centrifuged and mounted onto glass slides with Canada balsam. Glass shards were counted using a light microscope. The concentration of volcanic ash shards was determined as shard number per gram of dry sediment. Where shard concentrations were too high for counting (e.g., >10,000/gram of dry sediment) counts were extrapolated based on the number of traverses across the slide. This process was repeated at 1 cm intervals where high concentrations of glass shards were detected to determine the exact depth of the cryptotephra peak. The depth interval displaying a peak in volcanic glass shards was then re-sampled and subjected to density separation techniques to isolate the shards (as described in Blockley et al., 2005). The glass shards were then picked using a micromanipulator and embedded into an epoxy resin stub for geochemical characterization.

2.3. Grain-specific major and trace element analysis of tephra

The major element volcanic glass composition of the tephra was determined using a wavelength-dispersive JEOL JXA-8200 electron microprobe at the School of Archaeology, University of Oxford. Full analytical conditions are reported in Text S1. All glass data presented has been normalized to 100 wt% (water-free) for comparative purposes. Error bars on plots represent reproducibility, calculated as a 2× standard deviation of replicate analysis of MPI-DING StHs6/80-G reference glass (Jochum et al., 2006). The full glass dataset of the Canopus Hill cryptotephra and the secondary standard (MPI-DING reference glasses) data are reported in the Supplementary Dataset. Trace element analysis of volcanic glass shards from the Canopus Hill cryptotephra, and the Hudson 2 reference ash deposit from Lago Quijada, Chile (see Smith et al., 2019 for details) were performed using an Agilent 8900 triple quadrupole ICP-MS (ICP QQQ) coupled to a Resonetics 193 nm ArF excimer laser-ablation in the Department of Earth Sciences, Royal Holloway, University of London. The full analytical conditions are reported in Text S1. Full trace element glass datasets for the Canopus Hill cryptotephra and a Hudson 2 reference sample from Lago Quijada are provided in the Supplementary Dataset, along with the MPI-DING glass analyses (StHs6/80-G and ATHO-G).

2.4. Chronology

Fifteen radiocarbon ages and one ^{137}Cs age for the Canopus Hill peat sequence have previously been published in Thomas et al. (2018). These ^{14}C ages were derived using terrestrial plant macrofossils (fruits and leaves) and were given an acid–base–acid (ABA) pre-treatment. Samples were pretreated, combusted and graphitised in the University of Waikato AMS laboratory, and the $^{14}C/^{12}C$ measurements performed at the University of California at Irvine (UCI) on a NEC compact (1.5SDH) AMS system. The ^{14}C measurements were supplemented by ^{137}Cs measurements near the top of the profile to detect the onset of nuclear tests in the mid- 20th century, undertaken following standard techniques with measurements made using an ORTEC high-resolution, low-background coaxial germanium detector. For this study, an additional macrofossil sample (graminoid fragments) was extracted for ^{14}C dating from the sequence at 134 cm, to help constrain the existing age-depth model. The macrofossil was pre-treated, graphitised and measured on an Ionplus MICADAS at the University of New South Wales Chronos ^{14}Carbon-Cycle Facility (Turney et al., 2021). The sixteen radiocarbon and one ^{137}Cs ages are here recalibrated with SHCal20 (Hogg et al., 2020) and Bomb13SH1-2 (Hua et al., 2013), and an age-depth model recalculated using the P_sequence outlier analysis in OxCal 4.4 (Bronk Ramsey, 2008, 2017; Bronk Ramey, 2009; Bronk Ramsey and Lee, 2013). All radiocarbon ages for Canopus Hill are provided in Table S2.

3. Results and discussion

3.1. Tephrostratigraphy and chronology

Volcanic glass was found in varying abundances throughout the Canopus Hill sequence. Most shards were clear and appeared light pink, but a smaller proportion were darker. A distinct peak in volcanic glass occurred within the 136–140 cm and 140–144 cm intervals of the peat sequence (Fig. 2a; Fig S1). These intervals contained very high concentrations (>40,000 shards per gram) of clear/light pink volcanic glass shards. Further examination at 1 cm resolution indicated the peak in glass shards occurred between 139–140 cm (Fig. 2b.). The morphology of the shards at 139 cm were predominantly formed of clear, platy and cuspate shards. The age depth model for the Canopus Hill sequence is almost identical to that in Thomas et al. (2018), but now includes an additional macrofossil ^{14}C age from 134 cm (UNSW-1: 3752 ± 11 ^{14}C yrs BP) to provide an additional constraint for the tephra age. This new age model indicates the age of this cryptotephra deposit is 4265 ± 65 cal yrs BP (Fig. 2a), based off the midpoint of the cryptotephra at 139.5 cm.

3.2. Geochemical characterization and origin of the CP-139 cryptotephra

The CP-139 cryptotephra has a relatively heterogeneous volcanic glass composition that straddles the trachydacite-rhyolite boundary (67.3–70.6 wt% SiO_2; 8.9–9.7 wt% $Na_2O + K_2O$; Fig. 3a). These volcanic glasses also display a High-K calc-alkaline affinity (HKCA; 3.2–3.6 wt% K_2O). Using increasing SiO_2 as a fractionation index, the CP-139 glasses display a clear decrease in TiO_2, FeOt, MgO and CaO contents, whilst the K_2O content increases. Incompatible trace element contents of the CP-139 glasses reveal minor heterogeneity (e.g., 458–534 ppm Zr; 40–46 ppm Y; 891–946 ppm Ba) and show Light Rare Earth Element (LREE) enrichment relative to the Heavy Rare Earth Elements (HREE) (La/Yb = 9.6 ± 4.7 [2.s.d]).

The SiO_2 content of the CP-139 glass shards is relatively low compared to those of known widespread tephra units from large magnitude eruptions within the AVZ, for instance activity at Mt. Burney, Reclus and Aguilera (Fig. 3). Furthermore, widespread tephras from Mt. Burney and Reclus consist of glass compositions with a calc-alkaline affinity (CA; Smith et al., 2019) inconsistent with the source of the CP-139 tephra. Further north in the SVZ of the Andes, a number of volcanoes active during the Holocene have erupted HKCA deposits, including Quatrupillian, Sollipuli and Lanín (Fontijn et al., 2016). However, chronological inconsistency combined with a clear offset to higher Na_2O content in the CP-139 glass shards, relative to the products of these volcanoes at overlapping SiO_2 content, clearly preclude any potential correlations.

The CP-139 glass shards are indistinguishable at a major element level from the HKCA products of Hudson volcano in the SVZ, and specifically the mid-Holocene Hudson-2 (H2) that was chemically characterised in Smith et al. (2019). Near-source (55 km NE) major element glass data reported in Smith et al. (2019) was generated from well constrained H2 ash layers preserved in Lago Quijada and Lago Espejo that were previously identified by Weller et al. (2015). To test the strength of our major element correlation, we compared trace elements concentrations from CP-139 glass shards to new grain-specific data produced here for the H2 tephra at Lago Quijada. Trace element concentrations observed in CP-139 are consistent with the H2 tephra at Lago Quijada (Fig. 4), subtly differing from those of the Hudson-1 tephra (e.g., higher Ba, lower Sr content), and can be clearly distinguished from the less enriched incompatible trace element contents (e.g., Th, Y, Zr) of other widespread tephra units erupted within the AVZ (Del Carlo et al., 2018).

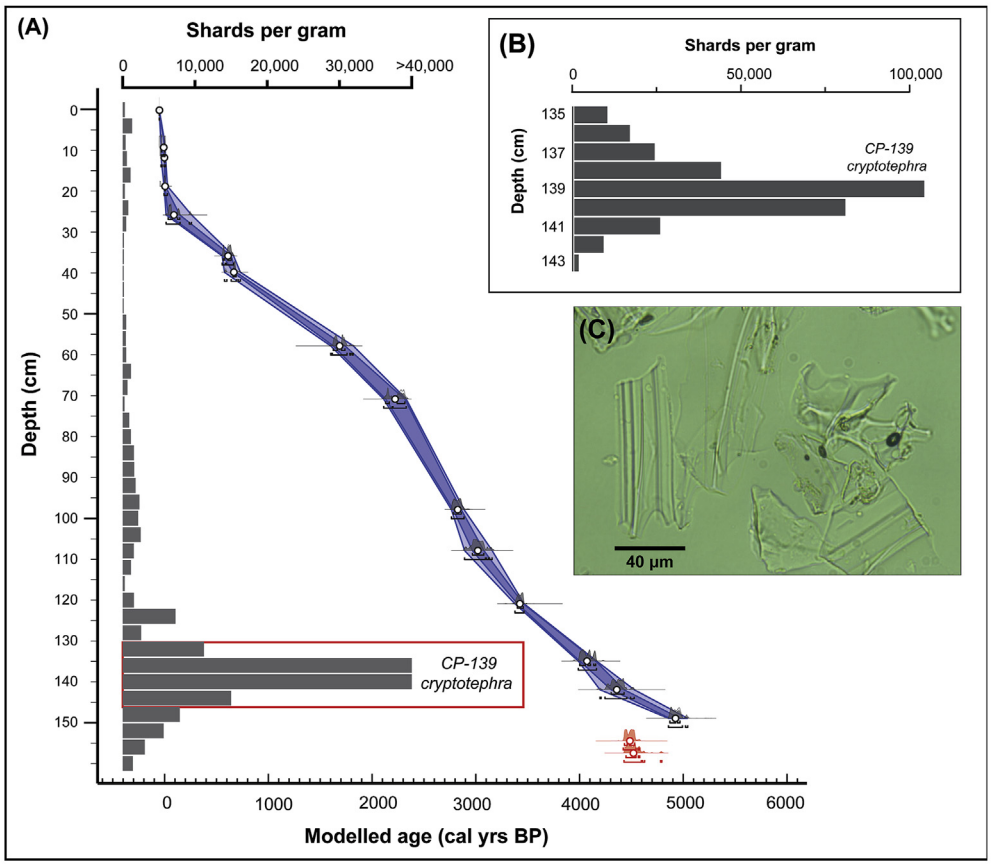

Fig. 2. Tephrostratigraphy of the Canopus Hill sequence. (A) Glass shard concentrations of samples spanning 4 cm intervals from 0 to 164 cm and the updated age depth model for the Canopus Hill peat sequence (Thomas et al., 2018). Probability distributions generated from the Bayesian age model are shown including the 1σ and 2σ age ranges (dark and light blue envelopes respectively). Red symbols indicate radiocarbon ages (outliers) not incorporated into the age model. (B) The glass shard concentrations between 135–143 cm at 1 cm intervals. (C) Image of volcanic shards from the CP-139×cryptotephra (light microscope, 20× magnification).

3.3. Implications

3.3.1. Dispersal and spatial extent of the H2 tephra

The first detailed report of H2 deposits by Naranjo and Stern (1998) was based on ICP-MS bulk tephra trace element chemistry and chrono-stratigraphy (Table S3). These showed an easterly dispersal with thicknesses that ranged from 40 cm at 55 km from the volcano, to <5 cm at 90 km from Mt. Hudson. H2 is widespread (>10 cm-thick) near the city of Coyhaique (80 km NE; sites 9–21 in Fig. 1) and has been reported 140 km to the SSE near Cochrane (<2 cm-thick; sites 5–8 in Fig. 1). H2 tephra is also reported at several distant localities 350–430 km SE, including the Los Toldos, Cerro Tres Tetas and La María archaeological sites (sites 23–25 in Fig. 1; Cardich, 1985; Paunero, 1994, 2000; Naranjo and Stern, 1998). Geochemical and chronological data supporting the identification of H2 tephra at these sites is provided in Tables S1, S3 and Fig. S2 (C.R Stern previously unpublished). Importantly, recent work has identified the H2 tephra 400 km east of source, within Atlantic coast aeolian sedimentary deposits near Caleta Olivia, Argentina (Zanchetta et al., 2021, Fig. 3). The occurrence of H2 as a cryptotephra (CP-139) in the Falkland Islands (1280 km SE of Mt. Hudson), verified by its grain-specific major and trace element glass compositions (Figs. 3–4), significantly extends the previously known distribution of this marker horizon (Fig. 1; Table S1).

The occurrence of H2 in the Falkland Islands also indicates that the widespread distribution of ash by high altitude winds may have been in a more SE direction than previously reported. According to Naranjo and Stern (1998), the dispersal axis of tephra fall from the H2 eruption, inferred from near-source deposits, was predominantly in an easterly direction (N85°E). However, satellite observations and simulations of phase II of the 1991 eruption - a possible analogue for the H2 eruption, indicate the ash plume was initially directed to the south before moving to the east and settling into a fixed SE direction (Kratzmann et al., 2010; Constantine et al., 2000). At its peak, the plume was elongated (1500 km SE) and reached a width of 370 km over the Falkland Islands (Scasso et al., 1994). Indeed, distal transport to the SE is supported by the reported H2 occurrences in the localities of Los Toldos, Cerro Tres Tetas and La María. These sites are also directly in line with the SE distribution of the Hudson 1991 tephra (Scasso et al., 1994). H2 deposits at these sites are >5 cm, which is similar to or greater than the thickness of the 1991 tephra that fell at these localities, according to the isopachs drawn by Scasso et al., (1994). This and the occurrence of H2 ash in the Falklands suggests that distal distribution of H2 tephra to the SE was as great, if not greater than during the 1991 eruption.

3.3.2. Age of the H2 eruption

Previous age estimates for the H2 eruption are summarised in Table S1. The commonly cited age (3600 BP; ~3.9 ka cal BP) was derived from ^{14}C ages of bulk organic soil, sediment and peat bracketing the tephra (Naranjo and Stern, 1998; Weller et al., 2018). However, most studies reporting H2 tephra have adopted this age without providing an independent estimate (e.g., Weller et al., 2015; Stern et al., 2016). Other age-estimates have been extrapolated from lake sediment cores using bulk radiometric dates (3535 BP; Haberle and Lumley, 1998) and bulk sediment samples

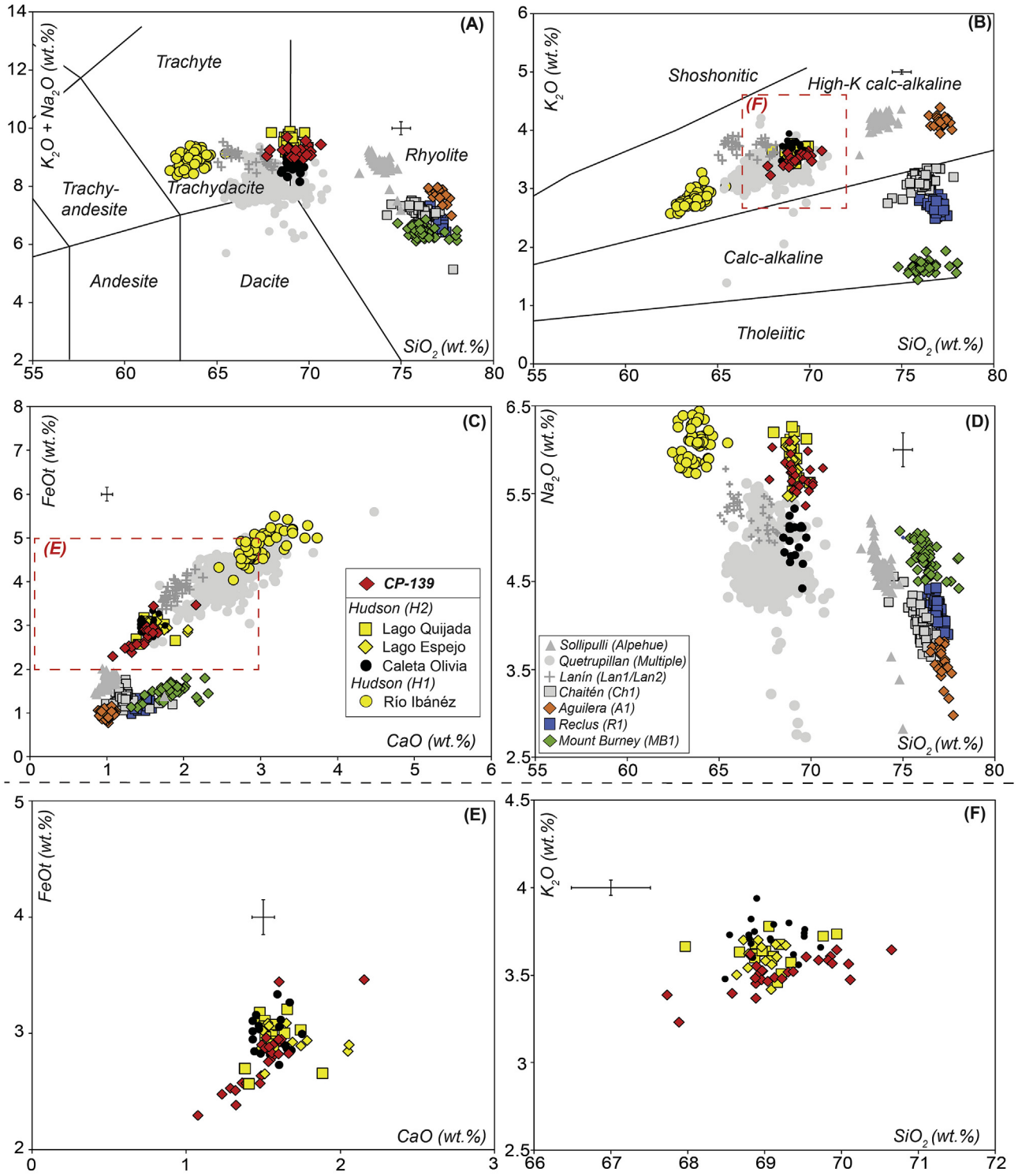

Fig. 3. Major element biplots comparing major elements of individual glass shards of CP-139 cryptotephra and widespread Holocene-Late Glacial tephra units originating from the volcanoes of the AVZ (Mt. Burney [MB1], Reclus [R1] and Aguilera [A1]) and the SVZ, (Hudson-1 [H1] and Hudson-2 [H2]) (data from Smith et al., 2019). The H2 major element glass data from Lago Quijada and Lago Espejo are reported in Smith et al. (2019), whilst the distal occurrence of Caleta Olivia, along the Argentine Atlantic coast, is reported in Zanchetta et al. (2021). The Caleta Olivia tephra shows subtle offsets in Na_2O content (Fig. 3D), however this is likely attributed to differing analytical operating conditions. Also shown are glass compositions of HKCA tephra layers from volcanoes located further north in the Southern Volcanic Zone including Chaitén, Lanín, Quetrupillan and Sollipulli (Fontijn et al., 2016). (A) Total alkali vs. Silica diagram follows Le Bas et al. (1986) and (B) SiO_2 vs K_2O classification diagram following Percerillo and Taylor (1976). Plots E-F illustrate H2 datasets only. Major and minor element glass data presented has been normalized to 100 wt% (water-free), and error bars represent 2 standard deviations of repeat analyses of the StHs6/80-G secondary standard run alongside CP-139.

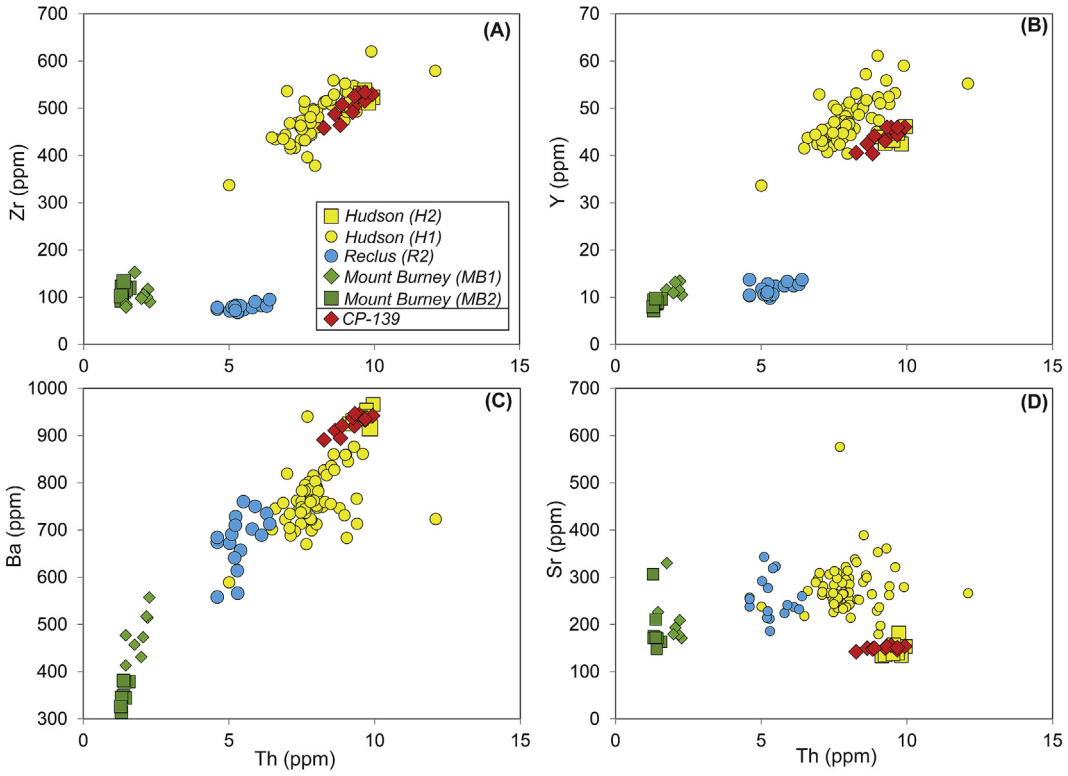

Fig. 4. Trace element biplots showing the concentrations of individual glass shards from the CP-139 cryptotephra (Falkland Islands), the mid-Holocene Hudson-2 (H2; Lago Quijada). Also shown are the trace element concentrations of the Hudson-1 (H1), Mt. Burney-1 (MB1), Mt. Burney-2 (MB2), and Reclus-2 (R2) tephra deposits, which relate to the Del Carlo et al. (2018) EO-2L, EO-2D, EO-1b and LA-IB samples. 2 × standard deviation error bars associated with repeat analyses of the StHs6/80-G secondary standard run alongside the CP-139 and H2 samples are typically smaller than the data symbols.

(~3970 cal BP; Elbert et al., 2013). Support for a slightly older age is provided at Lago Castor (3.97–4.11 ka cal BP; (Van Daele et al., 2016) and at Caleta Olivia (4058 ± 36 BP; 3967–4216 2σ cal range BP) for a shell dated directly below the H2 tephra in coastal aeolian deposits (Zanchetta et al., 2021).

Our age-depth model suggests the H2 tephra is slightly older (4265 ± 65 cal BP) than these previously reported age estimates. A possible explanation is that bulk sediment, that forms the majority of previous dating of the H2 eruption, may incorporate root material or downward vertical migration of microfossils by water movement/flow, both of which would result in a younger radiocarbon age determination. In contrast, the Canopus Hill age depth model was derived from terrestrial plant macrofossils. Dating short-lived terrestrial plant remains ensures that the assimilated atmospheric CO_2 is near-contemporaneous with the terrestrial environment, reflecting time of deposition (Lowe and Walker, 1997; Turney et al., 2000). Furthermore, the sampling site at Canopus Hill is a local topographic peak, which greatly reduces the potential for the redeposition of old material into the sediment sequence (Thomas et al., 2019). Indeed, previous dating of the Canopus Hill sequence found virtually identical probability distributions for paired ^{14}C ages for different peat fractions (bulk/macrofossil/fine) dated from the same depth (Thomas et al., 2019). This provides confidence that the Canopus Hill age depth model is robust and likely provides a more accurate age for the H2 eruption.

Given this older age of 4265 ± 65 cal BP, the H2 tephra may provide a key marker horizon for the Middle–Late Holocene Boundary (4.2 ka BP; Walker et al., 2012), an important climatostratigraphic boundary for which there are limited absolute time markers across the Southern Hemisphere. In South America, it marks the end of a period of widespread aridity that resulted in human population decline and/or collapse (Riris and Arroyo-Kalin, 2019). The H2 cryptotephra may therefore provide an important isochron for terrestrial and marine studies across SE Patagonia during a period of significant palaeoclimatic and prehistoric societal change across this region.

3.3.3. *Prospects for distal and ultra-distal correlations*

This discovery opens new possibilities for the investigation of Andean tephras in ultra-distal facies, including Antarctic ice cores, which have the potential to enable precise correlation of terrestrial, marine, and ice records (Dunbar et al., 2017; Di Roberto et al., 2019). Andean volcanoes, including Mt. Hudson, have been proposed as possible sources of tephra preserved in Antarctic ice cores (Narcisi et al., 2012; Kurbatov et al., 2006). For instance, Narcisi et al. (2012) proposed Mt. Hudson as the likely source of trachybasaltic (sample TD193; 2021 ± 66 BP) and rhyolitic (sample TD216; 2355 ± 54 BP) microtephras in the Talos Dome Core in East Antarctica. However, these correlations based on geochemistry and age have been questioned by Del Carlo et al. (2018) who suggest that circum-Antarctic volcanoes are equally feasible sources for these microtephras and that Andean sources should therefore be reconsidered. Despite this, Koffman et al. (2017) have correlated cryptotephra deposits in surface snow and shallow firn samples from the West Antarctic Ice Sheet to the 2011 CE Puyehue-Cordón Caulle eruption in Chile. This demonstrates that Andean tephra from modern eruptions can be transported to Antarctica. In summary, whilst there is limited evidence for Andean tephras in Antarctic ice cores, the potential for H2 cryptotephra to be found in Antarctica and across the Southern Ocean is an exciting prospect. We recommend future studies search for its presence across the sub-Antarctic islands and Antarctic Peninsula as a potentially useful

chronological marker.

4. Conclusion

The identification of a distal trachydacite-rhyolitic cryptotephra (CP-139) from the H2 eruption in the Falkland Islands greatly increases the previously known distribution of this key marker horizon. The high concentration of glass shards in our peat sequence suggests that the tephra may be more widespread than presently understood and may serve as an important isochron for the South Atlantic Ocean and possibly Antarctica. Our reference dataset of major and trace element glass composition can be used to identify the H2 tephra in other distal locations and is an important contribution in the development of a regional framework for the tephrostratigraphy of Patagonia. Finally, this research sets a precedent for further work into identifying South American cryptotephra in the sedimentary records of the Falkland Islands.

Author contributions

P. Panaretos: Conceptualization, Investigation, Data collection and Analysis, Writing – original draft. P. G. Albert: Conceptualization, data analysis, methodology, Writing - review & editing. Z. A. Thomas: Conceptualization, Supervision, Data analysis, Writing – review & editing. C. S.M. Turney: Conceptualization, Methodology, Supervision, Writing – review & editing. G. Jones: Data collection and analysis, Writing – review & editing. C. R. Stern: Data collection , resources, Writing - review & editing. A. N. Williams: Data collection, Writing - review & editing. V. C. Smith: Data collection, Writing - review & editing. A. G. Hogg: Data collection, Writing - review & editing. C. J. Manning: Data collection, Writing - review & editing.

Declaration of competing interest

The authors declare that they have no known competing financial interests or personal relationships that could have appeared to influence the work reported in this paper.

Acknowledgements

This project was supported by the Australian Research Council (grant no. DE200100907 and DP130104156). P. Panaretos was supported by a UNSW Summer Vacation Research Scholarship. P.G.A and G.J are funded through a UK Research and Innovation Future Leaders Fellowship (MR/S035478/1). We thank Rebecca Smith for providing constructive comments on an earlier version of this manuscript. We thank the Falkland Islands Government for permission to undertake sampling on the island (permit number: R07/2011).

Appendix A. Supplementary data

Supplementary data to this article can be found online at https://doi.org/10.1016/j.quascirev.2021.107074.

References

Alloway, B.V., Lowe, D.J., Larsen, G., Shane, P.A.R., Westgate, J.A., 2013. Tephrochronology. In: Elias, S.A., Mock, C.J. (Eds.), The Encyclopaedia of Quaternary Science, second ed., vol. 4. Elsevier, Amsterdam, pp. 277–304.

Blockley, S.P.E., Pyne-O'Donnell, S.D.F., Lowe, J.J., Matthews, I.P., Stone, A., Pollard, A.M., Turney, C.S.M., Molyneux, E.G., 2005. A new and less destructive laboratory procedure for the physical separation of distal glass tephra shards from sediments. Quat. Sci. Rev. 24 (16–17), 1952–1960. https://doi.org/10.1016/j.quascirev.2004.12.008.

Bronk Ramsey, C., 2017. OxCal Program, Version 4.3.

Bronk Ramsey, C., 2008. Deposition models for chronological records. Quat. Sci. Rev. 27, 42–60. https://doi.org/10.1016/j.quascirev.2007.01.019.

Bronk Ramsey, C., 2009. Dealing with outliers and offsets in radiocarbon dating. Radiocarbon 51, 1023–1045. https://doi.org/10.1017/S0033822200034093.

Bronk Ramsey, C., Lee, S., 2013. Recent and planned developments of the Program OxCal. Radiocarbon 55, 720–730. https://doi.org/10.2458/azu_js_rc.55.16215.

Cardich, A.R., 1985. Una fecha radiocarbónica más de la Cueva 3 de Los Toldos, Santa Cruz. Relaciones de la Sociedad Argentina de Antropología 16, 269–273.

Clark, R., Wilson, P., 1992. Occurrence and significance of ventifacts in the Falkland Islands, South Atlantic. Geogr. Ann. 74A, 35–46. https://doi.org/10.1080/04353676.1992.11880347.

Constantine, E.K., Bluth, G.J.S., Rose, W.I., 2000. TOMS and AVHRR observations of drifting volcanic clouds from the August 1991 eruptions of Cerro Hudson. In: Mouginis-Mark, P., Crisp, J., Fink, J. (Eds.), Remote Sensing of Active Volcanism, 45–64. Geophysical Monograph, Washington, DC.

Del Carlo, P., Di Roberto, A., D'Orazio, M., Petrelli, M., Angioletti, A., Zanchetta, G., Maggi, V., Daga, R., Nazzari, M., Rocchi, S., 2018. Late Glacial-Holocene tephra from southern Patagonia and Tierra del Fuego (Argentina, Chile): a complete textural and geochemical fingerprinting for distal correlations in the Southern Hemisphere. Quat. Sci. Rev. 195, 153–170. https://doi.org/10.1016/j.quascirev.2018.07.028.

Di Roberto, A., Colizza, E., Del Carlo, P., Petrelli, M., Finocchiaro, F., Kuhn, G., 2019. First marine cryptotephra in Antarctica found in sediments of the western Ross Sea correlates with englacial tephras and climate records. Sci. Rep. 9, 10628 https://doi.org/10.1038/s41598-019-47188-3, 2019.

Dugmore, A.J., 1989. Icelandic volcanic ash in Scotland. Scottish Geographical. Magazine 105, 168–172. https://doi.org/10.1080/14702548908554430.

Dunbar, N.W., Iverson, N.A., Van Eaton, A.R., Sigl, M., Alloway, B.V., Kurbatov, A.V., Mastin, L.G., McConnell, J.R., Wilson, C.J.N., 2017. New Zealand supereruption provides time marker for the Last Glacial Maximum in Antarctica. Sci. Rep. 7, 12238 https://doi.org/10.1038/s41598-017-11758-0.

Elbert, J., Wartenburger, R., von Gunten, L., Urrutia, R., Fischer, D., Fujak, M., Hamann, Y., Greber, N.D., Grosjean, M., 2013. Late Holocene air temperature variability reconstructed from the sediments of Laguna Escondida, Patagonia, Chile (45°30′S). Palaeogeogr. Palaeoclimatol. Palaeoecol. 369, 482–492. https://doi.org/10.1016/j.palaeo.2012.11.013.

Fagel, N., Alvarez, D., Namur, O., Devidal, J.L., Nuttin, L., Schmidt, S., Jana, P., Torrejon, F., Bertrand, S., Araneda, A., Urrutia, R., 2017. Lacustrine record of last millennia eruptions in Northern Chilean Patagonia (45–47° S). Holocene 27 (8), 1227–1251. https://doi.org/10.1177/0959683616687380.

Fontijn, K., Rawson, H., Van Daele, M., Moernaut, J., Abarzúa, A.M., Heirman, K., Bertrand, S., Pyle, D.M., Mather, T.A., De Batist, M., Naranjo, J.A., 2016. Synchronisation of sedimentary records using tephra: a postglacial tephrochronological model for the Chilean Lake District. Quat. Sci. Rev. 137, 234–254. https://doi.org/10.1016/j.quascirev.2016.02.015.

Fontijn, K., Lachowycz, S.M., Rawson, H., Pyle, D.M., Mather, T.A., Naranjo, J.A., Moreno-Roa, H., 2014. Late Quaternary tephrostratigraphy of southern Chile and Argentina. Quat. Sci. Rev. 89, 70–84. https://doi.org/10.1016/j.quascirev.2014.02.007.

Global Volcanism Program, 2020. Smithsonian Institution accessed date: 13 November 2020. https://volcano.si.edu/.

Haberle, S.G., Lumley, S.H., 1998. Age and origin of tephras recorded in postglacial lake sediments to the west of the southern Andes, 44°S to 47°S. J. Volcanol. Geoth. Res. 84, 239–256. https://doi.org/10.1016/S0377-0273(98)00037-7.

Hall, V.A., Wilson, P., Holmes, J., 2001. A preliminary tephra study of Holocene peats in the Falkland Islands. Dossiers de l'Archäol-Logis 1, 39–44.

Hogg, A.G., Heaton, T.J., Hua, Q., Palmer, J.G., Turney, C.S.M., Southon, J., Bayliss, A., Blackwell, P.G., Boswijk, G., Ramsey, C.B., Pearson, C., 2020. SHCal20 Southern Hemisphere calibration, 0–55,000 years cal BP. Radiocarbon 62 (4), 759–778. https://doi.org/10.1017/RDC.2020.59.

Hua, Q., Barbetti, M., Rakowski, A.Z., 2013. Atmospheric radiocarbon for the period 1950–2010. Radiocarbon 55, 2059–2072. https://doi.org/10.2458/azu_js_rc.v55i2.16177.

Jochum, K.P., Stoll, B., Herwig, K., Willbold, M., Hofmann, A.W., Amini, M., Aarburg, S., Abouchami, W., Hellebrand, E., Mocek, B., Raczek, I., 2006. MPI-DING reference glasses for in situ microanalysis: new reference values for element concentrations and isotope ratios. G-cubed 7 (2). https://doi.org/10.1029/2005GC001060.

Kearney, R., Albert, P.G., Staff, R.A., Pál, I., Veres, D., Magyari, E., Ramsey, C.B., 2018. Ultra-distal fine ash occurrences of the Icelandic Askja-S Plinian eruption deposits in Southern Carpathian lakes: new age constraints on a continental scale tephrostratigraphic marker. Quat. Sci. Rev. 188, 174–182. https://doi.org/10.1016/j.quascirev.2018.03.035.

Kilian, R., Hohner, M., Biester, H., Wallrabe-Adams, H.J., Stern, C.R., 2003. Holocene peat and lake sediment tephra record from the southernmost Chilean Andes (53-55 degrees S). Rev. Geol. Chile 30 (1), 23–37. https://doi.org/10.4067/S0716-02082003000100002.

Kilian, R., Lamy, F., 2012. A review of Glacial and Holocene paleoclimate records from southernmost Patagonia (49-55ºS). Quat. Sci. Rev. 53, 1–23. https://doi.org/10.1016/j.quascirev.2012.07.017.

Koffman, B.G., Dowd, E.G., Osterberg, E.C., Ferris, D.G., Hartman, L.H., Wheatley, S.D., Kurbatov, A.V., Wong, G.J., Markle, B.R., Dunbar, N.W., Kreutz, K.J., Yates, M., 2017. Rapid transport of ash and sulfate from the 2011 Puyehue-Cordón Caulle (Chile) eruption to West Antarctica. J. Geophys. Res. Atmos. 122, 8908–8920. https://doi.org/10.1002/2017JD026893.

Kratzmann, D.J., Carey, S.N., Fero, J., Scasso, R.A., Naranjo, J.A., 2010. Simulations of tephra dispersal from the 1991 explosive eruptions of Hudson volcano, Chile. J. Volcanol. Geoth. Res. 190, 337–352. https://doi.org/10.1016/j.jvolgeores.2009.11.021.

Kurbatov, A.V., Zielinski, G.A., Dunbar, N.W., Mayewski, P.A., Meyerson, E.A., Sneed, S.B., Taylor, K.C., 2006. A 12,000 year record of explosive volcanism in the Siple dome ice core, west Antarctica. J. Geophys. Res. 111, D12307 https://doi.org/10.1029/2005JD006072.

Lamy, F., Kilian, R., Arz, H.W., Francois, J.P., Kaiser, J., Prange, M., Steinke, T., 2010. Holocene changes in the position and intensity of the southern westerly wind belt. Nat. Geosci. 3 (10), 695–699. https://doi.org/10.1038/ngeo959.

Lane, C.S., Lowe, D.J., Blockley, S.P.E., Suzuki, T., Smith, V.C., 2017. Advancing tephrochronology as a global dating tool: applications in volcanology, archaeology, and paleoclimatic research. Quat. Geochronol. 40, 1–7. https://doi.org/10.1016/j.quageo.2017.04.003.

Le Bas, M.J., Le Maitre, R.W., Streckeisen, A., Zanettin, B., 1986. A chemical classification of volcanic rocks based on the total alkali-silica diagram. J. Petrol. 27, 745–750. https://doi.org/10.1093/petrology/27.3.745.

Lowe, D.J., 2011. Tephrochronology and its application: a review. Quat. Geochronol. 6, 107–153. https://doi.org/10.1016/j.quageo.2010.08.003.

Lowe, J.J., Walker, M.J.C., 1997. Reconstructing Quaternary Environments, second ed. Routledge.

Markgraf, V., Whitlock, C., Haberle, S., 2007. Vegetation and fire history during the last 18,000 cal yr B.P. In southern Patagonia: Mallín pollux, Coyhaique, province Aisén (45°41′30″ S, 71°50′30″ W, 640 m elevation). Palaeogeogr. Palaeoclimatol. Palaeoecol. 254, 492–507. https://doi.org/10.1016/j.palaeo.2007.07.008.

Monteath, A.J., Hughes, P.D.M., Wastegård, S., 2019. Evidence for distal transport of reworked Andean tephra: extending the cryptotephra framework from the Austral volcanic zone. Quat. Geochronol. 51, 64–71. https://doi.org/10.1016/j.quageo.2019.01.003.

Moreno, P.I., Vilanova, I., Villa-Martínez, R., Garreaud, R.D., Rojas, M., De Pol-Holz, R., 2014. Southern Annular Mode-like changes in southwestern Patagonia at centennial timescales over the last three millennia. Nat. Commun. 5, 4375. https://doi.org/10.1038/ncomms5375.

Naranjo, J.A., Stern, C.R., 1998. Holocene explosive activity of Hudson volcano, southern Andes. Bull. Volcanol. 59, 291–306. https://doi.org/10.1007/s004450050193.

Narcisi, B., Petit, J.R., Delmonte, B., Scarchilli, C., Stenni, B., 2012. A 16,000-yr tephra framework for the Antarctic ice sheet: a contribution from the new Talos Dome core. Quat. Sci. Rev. 49, 52–63. https://doi.org/10.1016/j.quascirev.2012.06.011.

Oppedal, L.T., van der Bilt, W.G., Balascio, N.L., Bakke, J., 2018. Patagonian ash on sub-Antarctic south Georgia: expanding the tephrostratigraphy of southern South America into the Atlantic sector of the Southern Ocean. J. Quat. Sci. 33 (5), 482–486. https://doi.org/10.1002/jqs.3035.

Otley, H., Munro, G., Clausen, A., Ingham, B., 2008. Falkland Islands State of the Environment Report 2008. Falkland Islands Government and Falklands Conservation, Stanley.

Paunero, R.S., 2000. Canadon Cueva de la Ventana: tefras del Holocene medio. In: Miotti, L., Paunero, R.S., Salemme, M., Cattaneo, G.R. (Eds.), Guia de camo de la visita a las localidades arqueologicas: La colonizacion del sur de America durante la tansicion Pleitoceno/Holoceno, pp. 113–118. Chapter 6.4.

Paunero, R.S., 1994. El sitio Cueva 1 de la localidad arqueologica Cerro Tres Tetas (Estancia San Rafael, provincial de Santa Cruz, Argentina). Anales de Arqueologia y Etnologia 48 (49), 3–90.

Peccerillo, A., Taylor, S.R., 1976. Geochemistry of Eocene calcalkaline volcanic rocks from Kastamonu area, Northern Turkey. Contributions to Mineralogy and Petrology 58, 39–63. https://doi.org/10.1007/BF00384745.

Pilcher, J.R., Hall, V.A., 1992. Towards a tephrochronology for the Holocene of the north of Ireland. Holocene 2, 255–259 https://doi.org/10.1177%2F095968369200200307.

Riris, P., Arroyo-Kalin, M., 2019. Widespread population decline in South America correlates with mid-Holocene climate change. Sci. Rep. 9, 6850. https://doi.org/10.1038/s41598-019-43086-w.

Scasso, R.A., Corbella, H., Tiberi, P., 1994. Sedimentological analysis of the tephra from the 12–15 August 1991 eruption of Hudson volcano. Bull. Volcanol. 56, 121–132. https://doi.org/10.1007/BF00304107.

Smith, R.E., Smith, V.C., Fontijn, K., Gebhardt, A.C., Wastegård, S., Zolitschka, B., Ohlendorf, C., Stern, C., Mayr, C., 2019. Refining the late quaternary tephrochronology for southern South America using the Laguna potrok Aike sedimentary record. Quat. Sci. Rev. 218, 137–156. https://doi.org/10.1016/j.quascirev.2019.06.001.

Smith, V.C., Costa, A., Aguirre-Díaz, G., Pedrazzi, D., Scifo, A., Plunkett, G., Poret, M., Tournigand, P.Y., Miles, D., Dee, M.W., McConnell, J.R., 2020. The magnitude and impact of the 431 CE Tierra Blanca Joven eruption of Ilopango, El Salvador. Proc. Natl. Acad. Sci. Unit. States Am. 117 (42), 26061–26068.

Stern, C.R., 1991. Mid-Holocene tephra on Tierra del Fuego (54°S) derived from the Hudson volcano (46°S): evidence for a large explosive eruption. Rev. Geol. Chile 18, 139–146.

Stern, C.R., 2004. Active Andean volcanism: its geologic and tectonic setting. Rev. Geol. Chile 31 (2), 1–51. https://doi.org/10.4067/S0716-02082004000200001.

Stern, C.R., 2008. Holocene tephrochronology record of large explosive eruptions in the southernmost Patagonian Andes. Bull. Volcanol. 70, 435–454. https://doi.org/10.1007/s00445-007-0148-z.

Stern, C.R., Moreno, P.I., Villa-Martinez, R., Sagredo, E.A., Prieto, A., Labarca, R., 2011. Evolution of ice-dammed proglacial lakes in Última Esperanza, Chile: implications from the late-glacial R1 eruption of Reclús volcano, Andean Austral Volcanic zone. Andean Geol. 38, 82–97.

Stern, C.R., Moreno Moncada, P., Henríquez, W.I., Villa Martínez, R., Sagredo, E., Aravena, J.C., Pol-Holz, R.D., 2016. Holocene tephrochronology around Cochrane (~47° S), southern Chile. Andean Geol. 43 (1), 1–19. https://doi.org/10.5027/andgeoV43n1-a01.

Stern, C.R., Aguerre, A.M., Andrieu, J.M., 2019. Obsidian in the Dásovich rock-shelter, Chubut, Argentina: implications for long-distance acquisition behavoirs. J. Archaeol. Sci.: Rep. 28, 102028 https://doi.org/10.1016/j.jasrep.2019.102028.

Thomas, Z.A., Jones, R.T., Fogwill, C.J., Hatton, J., Williams, A.N., Hogg, A., Mooney, S., Jones, P., Lister, D., Mayewski, P., Turney, C.S.M., 2018. Evidence for increased expression of the Amundsen sea low over the south Atlantic during the late Holocene. Clim. Past 14 (11), 1727–1738. https://doi.org/10.5194/cp-14-1727-2018.

Thomas, Z.A., Turney, C.S.M., Hogg, A.G., Williams, A.N., Fogwill, C.J., 2019. Investigating subantarctic ^{14}C ages of different peat components: site and sample selection for developing robust age models in dynamic landscapes. Radiocarbon 61 (4), 1009–1027. https://doi.org/10.1017/RDC.2019.54.

Turney, C.S.M., Jones, R.T., Fogwill, C., Hatton, J., Williams, A.N., Hogg, A., Thomas, Z.A., Palmer, J., Mooney, S., Reimer, R.W., 2016. A 250-year periodicity in Southern Hemisphere westerly winds over the last 2600 years. Clim. Past 12, 189–200. https://doi.org/10.5194/cp-12-189-2016.

Turney, C.S.M., Lowe, J.J., 2001. Tephrochronology. In: Last, W.M., Smol, J.P. (Eds.), Tracking Environmental Change Using Lake Sediments: Physical and Chemical Techniques. Kluwer Academic Press, Dordrecht, The Netherlands, pp. 451–471.

Turney, C.S.M., Coope, G.R., Harkness, D.D., Lowe, J.J., Walker, M.J.C., 2000. Implications for the dating of Wisconsinan (Weichselian) Late-glacial events of systematic radiocarbon age differences between terrestrial plant macrofossils from a site in SW Ireland. Quat. Res. 53, 114–121. https://doi.org/10.1006/qres.1999.2087.

Turney, C., Becerra-Valdivia, L., Sookdeo, A., Thomas, Z.A., Palmer, J., Haines, H.A., Cadd, H., Wacker, L., Baker, A., Anderson, M., Jacobsen, G., Meredith, K., Chinu, K., Bollhalder, S., Marjo, C., 2021. Radiocarbon protocols and first intercomparison results from the chronos ^{14}Carbon-cycle facility. University of New South Wales, Sydney, Australia. Radiocarbon 63, 1003–1023. https://doi.org/10.1017/RDC.2021.23.

Upton, J., Shaw, C.J., 2002. An overview of the oceanography and meteorology of the Falkland Islands. Aquatic conservation. Mar. Freshwater Ecosyst. 12, 15–25. https://doi.org/10.1002/aqc.496.

Van Daele, M., Bertrand, S., Meyer, I., Moernaut, J., Vandoorne, W., Siani, G., Tanghe, N., Ghazoui, Z., Pino, M., Urrutia, R., De Batist, M., 2016. Late Quaternary evolution of Lago Castor (Chile, 45.6°S): Timing of the deglaciation in northern Patagonia and evolution of the southern westerlies during the last 17 kyr. Quat. Sci. Rev. 133, 130–146. https://doi.org/10.1016/j.quascirev.2015.12.021.

Walker, M.J.C., Berkelhammer, M., Björck, S., Cwynar, L.C., Fisher, D.A., Long, A.J., Lowe, J.J., Newnham, R.M., Rasmussen, S.O., Weiss, H., 2012. Formal subdivision of the Holocene series/epoch: a discussion paper by a working group of INTIMATE (integration of ice-core, marine and terrestrial records) and the subcommission on quaternary stratigraphy (international commission on stratigraphy). J. Quat. Sci. 27, 649–659. https://doi.org/10.1002/jqs.2565.

Wastegård, S., Turney, C.S.M., Lowe, J.J., Roberts, S.J., 2000. New discoveries of the Vedde ash in southern Sweden and scotland. Boreas 29 (1), 72–78.

Weller, D.J., Miranda, C.G., Moreno, P.I., Villa-Martínez, R., Stern, C.R., 2015. Tephrochronology of the southernmost Andean southern volcanic zone, Chile. Bull. Volcanol. 77, 1–24. https://doi.org/10.1007/s00445-015-0991-2.

Weller, D.J., de Porras, M.E., Maldonado, A., Méndez, C., Stern, C.R., 2018. New age controls on the tephrochronology of the southernmost Andean southern volcanic zone, Chile. Quat. Res. 91 (1), 250–264. https://doi.org/10.1017/qua.2018.81.

Weller, D.J., Stern, C.R., 2018. Along-strike variability of primitive magmas (major and volatile elements) inferred from olivine-hosted melt inclusions, southernmost Andean Southern Volcanic Zone, Chile. Lithos 296–299, 233–244. https://doi.org/10.1016/j. lithos.2017.11.009.

Zanchetta, G., Pappalardo, M., Di Roberto, A., Bini, M., Arienzo, I., Isola, I., Boretto, G., Fuck, E., Mele, D., D'Orazio, M., Passariello, I., 2021. A Holocene tephra layer within coastal aeolian deposits north of Caleta Olivia (Santa Cruz Province, Argentina). Andean Geol. 48 (2), 267–280. https://doi.org/10.5027/andgeoV48n2-3290.